Probing Site-Specific Calmodulin Calcium and Lanthanide Affinity by Grafting

Yiming Ye, Hsiau-Wei Lee, Wei Yang, Sarah Shealy, and Jenny J. Yang*

Contribution from the Department of Chemistry, Center for Drug Design and Advanced Biotechnology, Georgia State University, Atlanta, Georgia 30303

Received November 30, 2004; E-mail: chejjy@panther.gsu.edu

Abstract: Ca^{2+} binding is essential for the biological functions of calmodulin (CaM) as a trigger/sensor protein to regulate many biological processes in the Ca^{2+}-signaling cascade. A challenge in understanding the mechanism of Ca^{2+} signaling is to obtain site-specific information about the Ca^{2+} binding properties of individual Ca^{2+}-binding sites of EF-hand proteins, especially for CaM. In this paper, we report the first estimation of the intrinsic Ca^{2+} affinities of the four EF-hand loops of calmoduin (I−IV) by individually grafting into the domain 1 of CD2. Taking advantage of the Trp residues in the host protein, we first determined metal-binding affinities for Tb^{3+}, Ca^{2+}, and La^{3+} for all four grafted EF-loops using Tb^{3+} aromatic resonance energy transfer. EF-loop I exhibits the strongest binding affinity for Ca^{2+}, La^{3+}, and Tb^{3+}, while EF-loop IV has the weakest metal-binding affinity. EF-loops I−IV of CaM have dissociation constants for Ca^{2+} of 34, 245, 185, and 814 μM, respectively, with the order I > III ≈ II > IV. These findings support a charge-ligand-balanced model in which both the number of negatively charged ligand residues and the balanced electrostatic dentate−dentate repulsion by the adjacent charged residues are two major determinants for the relative Ca^{2+}-binding affinities of EF-loops in CaM. Our grafting method provides a new strategy to obtain site-specific Ca^{2+} binding properties and a better estimation of the cooperativity and conformational change contributions of coupled EF-hand proteins.

1. Introduction

Calmodulin (CaM) is a ubiquitous and multifaceted intracellular Ca^{2+}-binding protein that regulates more than 100 different target proteins including phosphodiesterase, myosin light chain kinase, CaM kinase, calcineurin, nitric oxide synthase, and Ca^{2+}-gated channels (Figure 1).[1−5] The primary structure of CaM is highly conserved in all cell types and shares strong sequence and structure homology to troponin C (TnC), which is involved solely in the Ca^{2+}-dependent regulation of skeletal and heart muscle contraction.[6] Several CaM-like proteins have also been identified in the prokaryotic systems.[7,8] Currently, CaM is one of the most extensively recognized Ca^{2+}-binding proteins.

CaM contains two paired canonical EF-hand motifs of helix−loop−helix in two domains (Figure 1).[9] The 12-residue loop is responsible for the binding and coordination of the metal ions in the EF-hand loops (Figure 1).[10] The Ca^{2+} ion is coordinated to seven oxygen ligands from the side chains of residues 1, 3, 5, and 12, the mainchain carbonyl of position 7, and a bridged water at position 9. These oxygen atoms are spatially coordinated to Ca^{2+} in a pentagonal bipyramidal (or distored octahedral) configuration. Today, the EF-hand motif is one of the five most common protein motifs in animal cells, and more than 1000 EF-hand Ca^{2+}-binding proteins are found from prokaryotes to eukaryotes throughout the entire plant (Fungi included) and animal kingdoms.[11] According to their different biological roles, the Ca^{2+}-binding affinities of EF-hand proteins vary over a range of 10^6 fold or more.[6,10,12] Upon Ca^{2+} binding, the trigger proteins (Ca^{2+}-modulated proteins or sensor proteins such as CaM and troponin C) undergo a large conformational change and in turn regulate a vast number of target proteins.[13−15] In addition, the alteration of Ca^{2+}-binding affinities of these proteins has a strong influence on their functions in Ca^{2+} homeostasis, such as uptake, transport, and maintenance of proper Ca^{2+} concentration in the cellular environment.[12] One of the most interesting questions in Ca^{2+} signaling is how EF-hand proteins use the ubiquitous

(1) Lin, Y. M.; Liu, Y. P.; Cheung, W. Y. *J. Biol. Chem.* **1974**, *249*, 4943−4954.
(2) Klee, C. B. *Biochemistry* **1977**, *16*, 1017−1024.
(3) Richman, P. G.; Klee, C. B. *J. Biol. Chem.* **1979**, *254*, 5372−5376.
(4) Watterson, D. M.; Sharief, F.; Vanaman, T. C. *J. Biol. Chem.* **1980**, *255*, 962−975.
(5) Haiech, J.; Klee, C. B.; Demaille, J. G. *Biochemistry* **1981**, *20*, 3890−3897.
(6) Kawasaki, H.; Kretsinger, R. H. *Protein Profile* **1995**, *2*, 297−490.
(7) Michiels, J.; Xi, C.; Verhaert, J.; Vanderleyden, J. *Trends. Microbiol.* **2002**, *10*, 87−93.
(8) Rigden, D. J.; Jedrzejas, M. J.; Galperin, M. Y. *FEMS Microbiol. Lett.* **2003**, *221*, 103−110.
(9) Babu, Y. S.; Sack, J. S.; Greenhough, T. J.; Bugg, C. E.; Means, A. R.; Cook, W. J. *Nature* **1985**, *315*, 37−40.

(10) Falke, J. J.; Drake, S. K.; Hazard, A. L.; Peersen, O. B. *Q. Rev. Biophys.* **1994**, *27*, 219−290.
(11) Henikoff, S.; Greene, E. A.; Pietrokovski, S.; Bork, P.; Attwood, T. K.; Hood, L. *Science* **1997**, *278*, 609−614.
(12) Linse, S.; Forsen, S. *Adv. Second Messenger Phosphoprotein Res.* **1995**, *30*, 89−151.
(13) Ikura, M.; Clore, G. M.; Gronenborn, A. M.; Zhu, G.; Klee, C. B.; Bax, A. *Science* **1992**, *256*, 632−638.
(14) Zhang, M.; Tanaka, T.; Ikura, M. *Nat. Struct. Biol.* **1995**, *2*, 758−767.
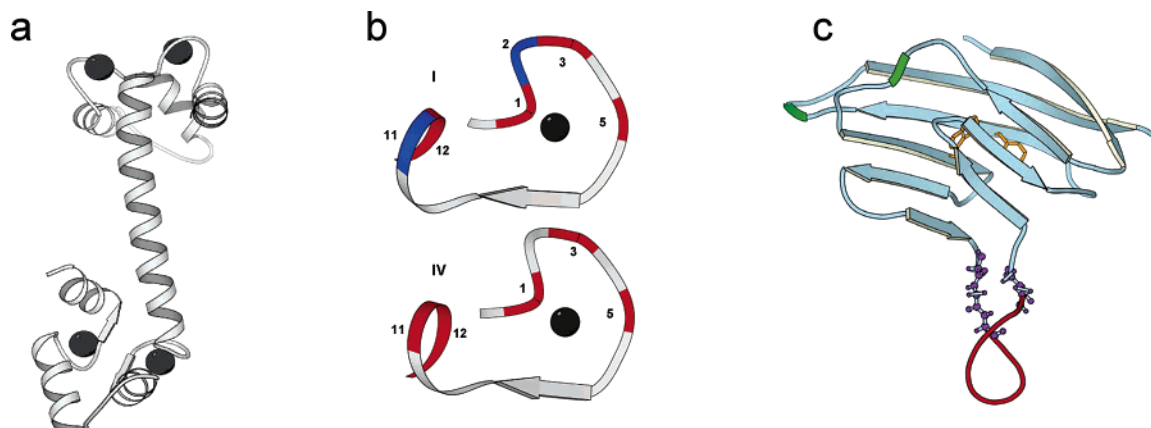(15) Chou, J. J.; Li, S.; Klee, C. B.; Bax, A. *Nat. Struct. Biol.* **2001**, *8*, 990−997.

Figure 1. (a) Three-dimensional structure of calmodulin (3cln).[17] Ca^{2+} ions are shown as dark spheres. Positions 1, 6, and 12 of the EF-loops are the most highly conserved with Asp, Gly, and Glu residues at each position, respectively. (b) Local structures of loop I (top) and IV (bottom) in CaM with negatively charged residues labeled in red and positively charged residues labeled in blue. Loop I contains two positively charged residues at loop position 2 and 11 to balance the negative repulsions, while loop IV contains an additional negatively charged residue at loop position 11. Hydrophobic residues at loop positions 7 and 8 form a small antiparallel beta-sheet with the neighboring Ca^{2+} binding loop. (c) The model structure of domain 1 of CD2 (CaM-CD2-III-5G-52) with EF-loop III grafted at position 52 connected by three and two gly residues at both ends of the sequence, respectively, based on the X-ray structure of CD2 (1hng) generated by the molecular mechanics, dynamics, and modeling program AMMP.[18] Three or two Gly residues (total 5G) are used to connect both termini of the Ca^{2+}-binding loops to provide the necessary flexibility to ensure native Ca^{2+} binding geometry and to minimize the influence of the host protein. Trp-32 and Tyr-76 are highlighted in yellow. This figure is prepared using MOLSCRIPT.[67]

EF-hand Ca^{2+}-binding motif to coordinate diverse cellular functions[10] with different Ca^{2+} affinities, especially how Ca^{2+} binding regulates the biological functions of trigger/sensor proteins such as CaM in the Ca^{2+}-signaling cascade.[16]

Site-specific metal binding properties of CaM and other EF-hand proteins are still limited and inclusive, although much progress has been made in attempting to understand the detailed mechanisms of Ca^{2+} binding and in obtaining structural information for the Ca^{2+}-free and -bound states of CaM and other EF-hand proteins. CaM was shown to bind Ca^{2+} in a stepwise mechanism.[5,19] The C-terminal of CaM was suggested to have a stronger Ca^{2+} binding affinity,[20] and similar results were observed for the two tryptically cleaved domains of CaM (TR_1C and TR_2C).[21-23] TR_2C (sites III and IV) has 6-fold stronger Ca^{2+} affinity than TR_1C (sites I and II).[24-26] On the other hand, sites I and II of CaM were suggested to have strong affinities for the Ca^{2+} analogues, such as Tb^{3+}, La^{3+}, and Eu^{3+}, with similar coordination properties to Ca^{2+}.[19,27-30] It is quite puzzling why sites III and IV from the C-terminal of CaM prefer to bind Ca^{2+}, while sites I and II prefer to bind Ln^{3+}. It has

also been reported that CaM exhibits different binding preferences for different Ln^{3+} ions.[31] Obtaining the site-specific metal binding affinity of CaM and other EF-hand proteins was carried out using various peptide fragments and different kinds or combinations of mutations at the Ca^{2+} binding loop.[32-34] Due to the limitation of cooperative binding and contribution of conformational entropy, the relative binding affinities of Ca^{2+} and its Ln^{3+} analogues of each binding loop of CaM have yet to be clearly described.

We have developed an approach for obtaining the site-specific Ca^{2+}-binding affinity of EF-hand proteins by grafting the EF-hand Ca^{2+}-binding loop III of CaM into a scaffold protein.[35-37] We have shown that domain 1 of the cell adhesion protein CD2 (CD2) is an excellent scaffold protein.[38] It retains its native structure after the insertion of the EF-hand Ca^{2+}-binding motif in both the absence and presence of Ca^{2+} ions. This characteristic is important, since it provides the foundation for measuring the intrinsic Ca^{2+} binding affinity with minimized contribution of protein conformational change.[35] In addition, the aromatic residues in CD2 enable us to obtain Tb^{3+} affinity of the grafted EF-loops using FRET. We have also optimized the length of two glycine linkers used to attach EF-loop III of CaM in CD2 to allow nativelike Ca^{2+}-binding properties. Further, we have demonstrated that the metal-binding affinity of the grafted EF-loop III is independent of the host protein environment.[36] Moreover, the grafted EF-hand Ca^{2+}-binding loop was stable as a monomer without coupling and pairing with another EF-

(16) Nelson, M. R.; Chazin, W. J. *BioMetals* **1998**, *11*, 297−318.
(17) Babu, Y. S.; Bugg, C. E.; Cook, W. J. *J. Mol. Biol.* **1988**, *204*, 191−204.
(18) Harrison, R. W.; Chatterjee, D.; Weber, I. T. *Proteins* **1995**, *23*, 463−471.
(19) Wang, C. L.; Aquaron, R. R.; Leavis, P. C.; Gergely, J. *Eur. J. Biochem.* **1982**, *124*, 7−12.
(20) Seamon, K. B. *Biochemistry* **1980**, *19*, 207−215.
(21) Dalgarno, D. C.; Klevit, R. E.; Levine, B. A.; Williams, R. J. P.; Dobrowolski, Z.; Drabikowski, W. *Eur. J. Biochem.* **1984**, *138*, 281−289.
(22) Aulabaugh, A.; Niemczura, W. P.; Blundell, T. L.; Gibbons, W. A. *Eur. J. Biochem.* **1984**, *143*, 409−418.
(23) Aulabaugh, A.; Niemczura, W. P.; Gibbons, W. A. *Biochem. Biophys. Res. Commun.* **1984**, *118*, 225−232.
(24) Martin, S. R.; Andersson Teleman, A.; Bayley, P. M.; Drakenberg, T.; Forsen, S. *Eur. J. Biochem.* **1985**, *151*, 543−550.
(25) Linse, S.; Helmersson, A.; Forsen, S. *J. Biol. Chem.* **1991**, *266*, 8050−8054.
(26) Waltersson, Y.; Linse, S.; Brodin, P.; Grundstrom, T. *Biochemistry* **1993**, *32*, 7866−7871.
(27) Kilhoffer, M. C.; Gerard, D.; Demaille, J. G. *FEBS Lett.* **1980**, *120*, 99−103.
(28) Wallace, R. W.; Tallant, E. A.; Dockter, M. E.; Cheung, W. Y. *J. Biol. Chem.* **1982**, *257*, 1845−1854.
(29) Wang, C. L.; Leavis, P. C.; Gergely, J. *Biochemistry* **1984**, *23*, 6410−6415.
(30) Biekofsky, R. R.; Muskett, F. W.; Schmidt, J. M.; Martin, S. R.; Browne, J. P.; Bayley, P. M.; Feeney, J. *FEBS Lett.* **1999**, *460*, 519−526.

(31) Buccigross, J. M.; Nelson, D. J. *Biochem. Biophys. Res. Commun.* **1986**, *138*, 1243−1249.
(32) Maune, J. F.; Beckingham, K.; Martin, S. R.; Bayley, P. M. *Biochemistry* **1992**, *31*, 7779−7786.
(33) Martin, S. R.; Maune, J. F.; Beckingham, K.; Bayley, P. M. *Eur. J. Biochem.* **1992**, *205*, 1107−1114.
(34) Starovasnik, M. A.; Su, D. R.; Beckingham, K.; Klevit, R. E. *Protein Sci.* **1992**, *1*, 245−253.
(35) Ye, Y. M.; Lee, H. W.; Yang, W.; Shealy, S. J.; Wilkins, A. L.; Liu, Z. R.; Yang, J. J. *Protein Eng.* **2001**, *14*, 1001−1003.
(36) Ye, Y. M.; Lee, H. W.; Yang, W.; Shealy, S. J.; Torshin, I.; Harrison, R.; Yang, J. J. *Protein Eng.* **2003**, *16*, 429−434.
(37) Yang, J. J.; Gawthrop, A.; Ye, Y. *Protein Pept. Lett.* **2003**, *10*, 331−345.
(38) Yang, J. J.; Ye, Y. M.; Carroll, A. R.; Yang, W.; Lee, H. W. *Curr. Protein Pept. Sci.* **2001**, *2*, 1−17.

hand motif as observed in natural EF-hand proteins.[39] Therefore, this established method allows us to obtain the intrinsic Ca^{2+} affinity and to estimate the contribution of the cooperativity from coupled EF-hand motifs of CaM.

In this study, we examine the relative metal binding affinities of the four EF-hand loops from CaM using our grafting methodology. Four EF-hand Ca^{2+} binding loops of CaM have been grafted into domain 1 of CD2 between the beta-strands C″ and D at amino acid position 52, denoted as CaM-CD2-I-5G-52, CaM-CD2-II-5G-52, CaM-CD2-III-5G-52, and CaM-CD2-IV-5G-52, respectively. Figure 1 shows the schematic representation of domain 1 of CD2 with the insertion of the EF-hand Ca^{2+}-binding loop III of CaM.

2. Experimental Methods

2.1. Protein Engineering, Expression, and Purification. The four EF-loops of calmodulin were inserted into domain 1 of rat CD2 (residue 1−99) using the same cloning strategy as that for CaM-CD2-III-5G-52.[36] Recombinant CD2 variants were expressed in LB medium as a fusion construct with the enzyme glutathione-*S*-transferase (GST) of *Schistosoma japonicum* in a pGEX plasmid vector transformed into *E. coli* BL21 (DE3). CD2 variants were first purified as a GST fusion protein using glutathione sepharose 4B beads (Pharmacia). After being cleaved by thrombin, CD2 variants were further purified using Superdex 75 and Hitrap SP columns (Pharmacia) in 10 mM Tris-HCl. The molecular weights of the CD2 variants were confirmed by MALDI TOF and electrospray mass spectrometry. The concentration of CD2 variants was measured by its absorption at 280 nm with an extinction coefficient of CD2 $\epsilon_{280} = 11\,700$ M^{-1} cm^{-1}.[40] All of the protein samples and buffers used were treated by Chelex-100 (Bio-rad) or Ca^{2+} sponge-S (Molecular Probes) to remove background Ca^{2+}.

2.2. Circular Dichroism. The CD spectra were measured using a Jasco-810 spectropolarimeter. A CD cell with a 10 mm light-path was used for far UV CD spectra. All spectra were the average of four or eight scans with a scan rate of 100 nm/min. The protein concentrations were 2−6 μM. All solutions were prepared using 10 mM Tris−10 mM KCl at pH 7.4 that was prepurified on Chelex-100 (Bio-Rad) or Ca^{2+} sponge chelating columns.

2.3. Rhodamine-5N (Rhod-5N) Fluorescence Competition. All fluorescence experiments were performed using a PTI lifetime fluorimeter equipped with a temperature-controlled water bath (Neslab 110) at 25 °C with a 1-cm path length fluorescence cell. The Ca^{2+} affinities of CD2 variants were also measured by competition with Rhod-5N (Molecular Probes) fluorescence. Rhod-5N is a Ca^{2+} dye whose fluorescence (emission at 580 nm while excitation at 552 nm) increases upon Ca^{2+} binding. The emission spectra of 20 μM of Rhod-5N in the absence and presence of 0.05−0.10 mM CD2 variant proteins were collected as a function of Ca^{2+} concentration in 10 mM Tris−10 mM KCl at pH 7.4 (excited at 552 nm) with a 1-cm path length. To compare our data to the reported results, different buffer conditions have been used.[25] Fluorescence intensity in the absence and presence of proteins was fitted using the program Specfit/32 (Spectrum Software Associates).

2.4. Intrinsic Trp Fluorescence. The emission of 2 μM protein concentration was monitored from 300 to 400 nm with the excitation wavelength at 283 nm. The slit widths for excitation and emission were 4 and 8 nm, respectively. The effect of metal ions on the Trp fluorescence was investigated by gradually adding stock solutions of La^{3+} (1.0 or 10 mM) with 2 μM protein into a 2 μM protein sample in 10 mM Tris−10 mM KCl at pH 6.9. An incubation time of 10−15 min was used to allow equilibration between each measurement. Light bleaching was minimized by closing the excitation shutter during

incubation. The net change of the Trp fluorescence for the CD2 variants due to La^{3+} binding was calculated by normalizing for the contribution of quenching using the same concentration of CD2 at each metal concentration.

2.5. Aromatic Residue-Sensitized Tb^{3+} Energy Transfer. Aromatic residue-sensitized Tb^{3+} energy transfer was carried out with a protein concentration of 2−4 μM in 20 mM PIPES−10 mM KCl at pH 6.8 at 25 °C. Tb^{3+} emission fluorescence spectra were acquired from 500 to 600 nm with excitation at 283 or 292 nm. The slit widths for excitation and emission were 8 and 12 nm, respectively. A glass filter with a long pass of >340 nm was used to avoid secondary Raleigh scattering. Samples with different Tb^{3+} concentrations were prepared by gradually adding Tb^{3+} stock solutions (0.1 or 1.0 mM with the same concentration of titrating protein to avoid the dilution effect) to the protein solution. An equilibrium time of 10−20 min was used between each titration. The competition of La^{3+} or Ca^{2+} for the Tb^{3+}-binding pocket using Tb^{3+} fluorescence enhancement was carried out using 2−4 μM protein with 30 μM Tb^{3+} equilibrated with 0.10 mM La^{3+} or with 10 mM Ca^{2+} in 10 mM Tris−10 mM KCl at pH 7.4 for 1 h. Tb^{3+} emission signals in the presence and absence of protein (residual signal) at 545 nm were calculated using published methods.[35] The K_d values of proteins were calculated by fitting the titration curves by assuming that the changes are from both the specific and nonspecific binding using the following equation:

$$\Delta S = \Delta S_{max} \times$$
$$\frac{([P]_T + [M]_T + K_d) - \sqrt{([P]_T + [M]_T + K_d)^2 - 4[P]_T[M]_T}}{2[P]_T} +$$
$$C \times [M]_T$$

where ΔS and ΔS_{max} are the signal change and the total signal change from the specific binding, respectively; C is the contribution from the nonspecific binding; and $[M]_T$ and $[P]_T$ are the total concentrations of metal ions and protein, respectively. The Tb^{3+} fluorescence enhancements with CD2 variants in the presence of Ca^{2+} or La^{3+} were calculated by subtracting the Tb^{3+} fluorescence in the presence of Ca^{2+} or La^{3+} in the absence of the protein. La^{3+} and Tb^{3+} binding affinities of proteins were calculated using published methods.[35]

2.6. 1D ^{1}H NMR. NMR samples were prepared by diluting the proteins in 10 mM Tris−10 mM KCl, 10% D_2O at pH 7.4. Protein concentrations varied between 110 and 170 μM. Spectra widths of 6600 and 8000 Hz were used for 1D NMR at 500 and 600 MHz NMR, respectively. A modified WATERGATE pulse sequence was used for 1D NMR with 16 K complex data points at 25 °C. Different amounts of Ca^{2+} and La^{3+} (10−40 μL of 1 mM, 10 mM, and 1 M metal ion stock solutions at pH 7.4) were gradually added into the NMR sample tube. The 1D NMR spectra at different metal ion concentrations were the average of 1024 scans. Samples were incubated with the addition of metal ions about 30 min before the next acquisition. The data were processed with the program FELIX98 (MSI) with a squared sinebell window function shifted over 75°. Postacquisition suppression of the water signal was achieved by a Gaussian deconvolution function with a width of 20.

2.7. Mass Spectrometry. Metal uptake by the proteins was analyzed by mass spectrometry using the electrospray technique. A Micromass Quattro LC instrument was used to acquire the data in positive ion mode by syringe pump infusion of the protein solutions at a flow rate of 10 μL/min. All samples were measured in either 100% water or 10 mM Tris buffer at pH 7.4 to maintain nondenaturing conditions. $CaCl_2$ or $LaCl_3$ was added in 0−200 molar excess to the protein concentration to observe specific binding. Both ions bind with 1:1 stoichiometry such that the metal-bound mass peak was observed at either M + 38 for Ca^{2+} or M + 137 for La^{3+}.

(39) Lee, H. W.; Yang, W.; Ye, Y.; Liu, Z. R.; Glushka, J.; Yang, J. J. *Biochim. Biophys. Acta* **2002**, *1598*, 80−87.
(40) Driscoll, P. C.; Cyster, J. G.; Campbell, I. D.; Williams, A. F. *Nature* **1991**, *353*, 762−765.
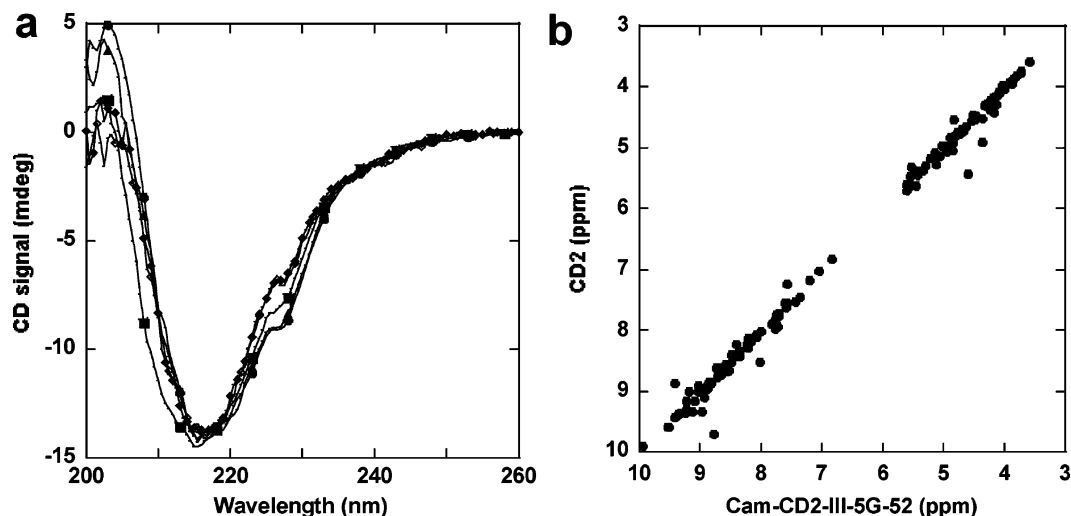
Figure 2. (a) Far UV CD spectra of CaM-CD2-I-5G-52 (●), CaM-CD2-II-5G-52 (■), CaM-CD2-III-5G-52 (◆), CaM-CD2-IV-5G-52 (▲) in the presence of 1 mM EGTA, and CaM-CD2-III-5G-52 (◇) in the presence of 1 mM Ca^{2+} in 10 mM Tris−10 mM KCl, pH 7.4 at 25 °C. (b) Comparison of the chemical shifts of CD2 vs CaM-CD2-III-5G-52 in 10 mM Tris−10 mM KCl, pH 7.4 and 25 °C. The majority of the $C\alpha$ and amide proton chemical shifts of CaM-CD2-III-5G-52 are similar to the chemical shifts of CD2. These results suggest that the integrity and packing of the host protein frame are maintained after the insertion of the Ca^{2+}-binding loop from CaM.

3. Results

3.1. Native Structure of the Host Protein. The effect of the insertion of the EF-loop and metal binding on the conformations of CD2 were monitored by far-UV circular dichroism (CD), fluorescence, and NMR. As shown in Figure 2, the CD spectra of CD2 variants are similar to that of CD2, suggesting that the insertion of EF-loops with glycine linkers into CD2 does not change the native structure in the host protein. This is further supported by the close similarity of the Trp emission fluorescence (see Figure 1, Supporting Information) and ^{1}H NMR spectra (see Figure 2, Supporting Information) of CD2 variants to those of CD2. The majority of the dispersed signals in the fingerprint regions of the TOCSY spectra of the CD2 variants are located at the same positions as those of CD2 (data not shown). As shown in Figure 2b, the chemical shifts of CaM-CD2-III-5G-52 are very similar to those of CD2, suggesting that the integrity and packing of the host protein are maintained after the insertion of the Ca^{2+}-binding loop from CaM. In addition, there is no alteration of the emission maximum of the Trp spectra for any CD2 variant, although the Trp fluorescence signal is reduced about 10% and 30% upon addition of 1 mM Ca^{2+} and La^{3+}, respectively. Furthermore, there are no noticeable changes in CD or in the overall patterns of 1D NMR spectra for the side chain and amide regions upon the addition of Ca^{2+}. The majority of the chemical shifts of the NMR resonances for the CD2 variants that are similar to CD2 remain the same upon addition of Ca^{2+}. Collectively, the overall conformation of the host protein is not perturbed by the insertion of the EF-loops and the addition of metal ions.

3.2. Formation of 1:1 Metal/Protein Complex Determined by Mass Spectrometry. Figure 3 shows the electrospray mass spectra of EF-loops in CD2 in the presence of a 20 molar excess of Ca^{2+}. The molecular masses of four CD2 variants in the absence and presence of excess Ca^{2+} and Ln^{3+} are listed in Table 1. The molecular masses of the apo-form of these proteins agree well with the calculated molecular masses. In the presence of Ca^{2+}, a new peak with an addition mass of 38 ± 1 Da was observed for all four grafted EF-loops, which corresponds to

the molecular masses of the Ca^{2+}-loaded forms. No other additional mass peaks were detected. Similar results were observed for the addition of La^{3+} (Table 1). Therefore, mass spectrometry reveals the metal binding ability of the CD2 variants and the formation of 1:1 protein/metal complexes.

3.3. Monitoring Ca^{2+}-Binding Affinity by Dye Competition. The Ca^{2+} binding affinities of four EF-loops in CD2 were measured by monitoring the fluorescence change of the Ca^{2+} dye Rhod-5N in the presence of 50 μM protein. The fluorescence emission at 580 nm of Rhod-5N is greatly enhanced upon Ca^{2+} binding upon excitation at 552 nm (see Figure 3, Supporting Information). Ca^{2+}-Rhod-5N has a K_d of 104 μM in 10 mM Tris−10 mM KCl, pH 7.4. In the presence of the CD2 variants, a delay of the Rhod-5N fluorescence increase has been observed. This effect is not observed in the presence of CD2. The Ca^{2+} affinities for the four CD2 variants determined by the competition assay are summarized in Table 1 and agree well with the affinities obtained by monitoring the chemical shift changes by NMR.[35]

3.4. Monitoring Metal Binding by Fluorescence Resonance Energy Transfer (FRET). Tb^{3+} binding to the N-terminal EF-loops of CaM were not directly monitored by fluorescence due to the lack of aromatic residues in the EF-loops of the N-terminal domain. The scaffold protein CD2 contains Trp-32 within 15 Å of the grafted EF-hand motifs. Such proximity allows us to use FRET to monitor metal binding. Figure 4 shows that the Tb^{3+} emission signal is significantly enhanced upon the addition of CaM-CD2-IV-5G-52 when excited at 283 nm. Similarly, CD2 variants with grafted EF-loops I, II, and III enhance Tb^{3+} emission at 545 nm. On the other hand, CD2 does not enhance Tb^{3+} fluorescence, although it contains the same number of Trp residues. These data suggest that the observed Tb^{3+} enhancement results from the binding of Tb^{3+} to the inserted EF-hand metal binding sites. Since there is one Tyr residue located in EF-loops III and IV of CaM, we used the same concentration (5 μM) of each protein in the presence of 100 μM Tb^{3+} to verify the origin of Tb^{3+} fluorescence enhancement. As shown in Figure 4b, Tb^{3+} enhancement by loop III or IV is about 30−
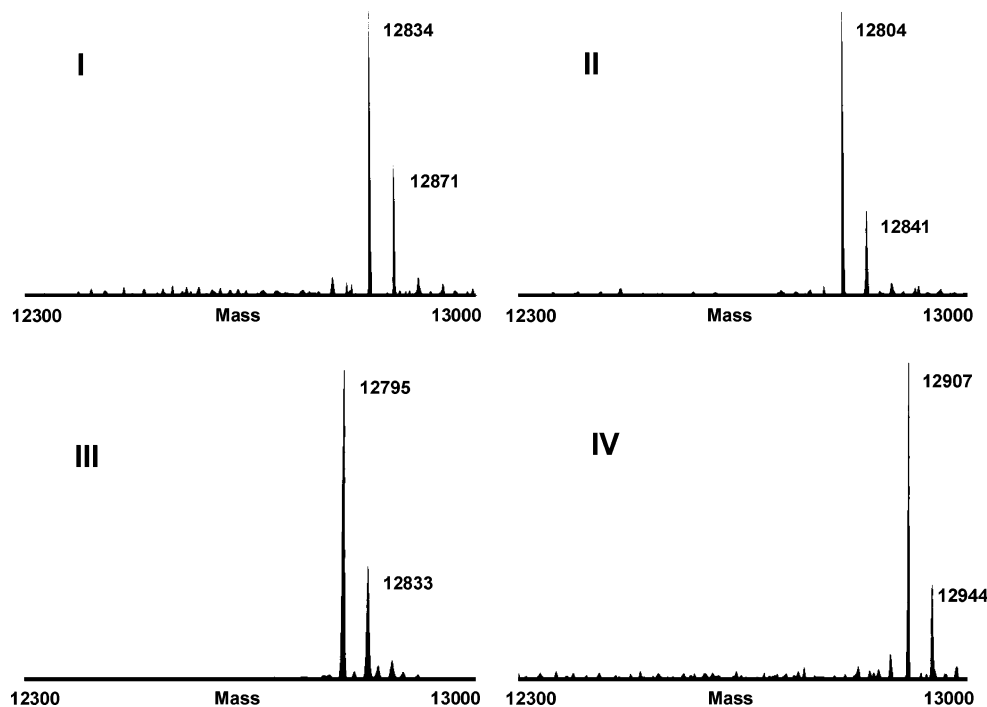
Figure 3. Electrospray mass spectra of CD2 with four grafted EF-loops in the presence of a 20-fold molar excess of CaCl$_2$.

Table 1. Mass and the Metal Binding Affinities of CD2 Variants with Inserted EF-Loops of CaM

	site I	site II	site III	site IV
mass (daltons)				
without metal	12 834	12 804	12 795	12 907
with Ca	12 871	12 841	12 833	12 944
with La	12 971	12 941	12 932	13 044
K_d (μM)				
Ca[a]	34 ± 9	245 ± 6	185 ± 30	814 ± 38
Ca[b]	37 ± 3	120 ± 10	135 ± 10	365 ± 35
Ca[c]	125 ± 15	400 ± 20	435 ± 30	1060 ± 200
Ca[d]	0.28 ± 0.03 and 0.29 ± 0.03		0.13 ± 0.02 and 0.020 ± 0.002	
Tb[e]	5 ± 1	25 ± 6	20 ± 6	72 ± 10
La[e]	12 ± 4	32 ± 6	40 ± 7	120 ± 30

[a] In 10 mM Tris−10 mM KCl, pH 7.4. [b] In 2 mM Tris, pH 7.5, without KCl. [c] In 2 mM Tris, pH 7.5, 150 mM KCl. [d] In 2 mM Tris, pH 7.5, low salt, in TR$_1$C (for site I and II) or TR$_2$C (for site III and IV).[25] [e] In 20 mM PIPES−10 mM KCl, pH 6.8.

40% greater than that by loops I and II. Thus, the donors for energy transfer for both CaM-CD2-III-5G-52 and CaM-CD2-IV-5G-52 are likely the Trp-32 in the host protein and the Tyr located in the EF-loop.

The measurements of Tb^{3+}-binding affinities of CD2 variants were carried out using the Tb^{3+} fluorescence enhancement as a function of total Tb^{3+} concentration. Figure 4c shows that the Tb^{3+} fluorescence enhancement in the presence of CaM-CD2-I-5G-52 exhibits an increase with the addition of Tb^{3+} when excited at 283 nm. The change of Tb^{3+} fluorescence intensity at 545 nm fits well with the binding equation, assuming a 1:1 protein/Tb^{3+}complex. The K_d's for the CD2 variants are 5, 25, 20, and 72 μM for sites I, II, III, and IV, respectively. In addition, the Tb^{3+} fluorescence enhancement at 545 nm decreases in the presence of excess La^{3+} or Ca^{2+} (Figure 4), suggesting that both La^{3+} and Ca^{2+} compete with Tb^{3+} to bind to the inserted EF-hand loops. The La^{3+}-binding affinities of CD2 variants were obtained by monitoring intrinsic Trp fluorescence change as a function of La^{3+} concentration.[36] The dissociation constants for La^{3+} are 12, 32, 40, and 120 μM for the sites I−IV, respectively. The isolated EF-loops inserted

in CD2 exhibit similar relative metal binding preferences for Ca^{2+} to that for Ln^{3+}, which is different from the behavior in intact CaM. Ln^{3+} binds to the N-terminal of calmodulin first, while Ca^{2+} binds to the C-terminal domain of the protein first.[29]

4. Discussion

4.1. Obtaining Site Specific Affinity of EF-Hand Proteins. As shown in Figure 5, the free energy change ΔG measured by any method of the binding process of the proteins with two coupled EF-hand binding sites (site I and II) can be described as the sum of the intrinsic energy change of each binding process ($\Delta G_{intr1} + \Delta G_{intr2}$), the contribution from the conformational change (ΔG_{conf}) from the surroundings, and the contribution from the cooperativity between the two metal binding sites (ΔG_{coop})

$$\Delta G = \Delta G_{intr1} + \Delta G_{intr2} + \Delta G_{coop} + \Delta G_{conf} \quad (1)$$

$$\Delta G_{coop} + \Delta G_{conf} = RT \ln \frac{K_{macro1}K_{macro2}}{K_{micro1}K_{micro2}} \quad (2)$$
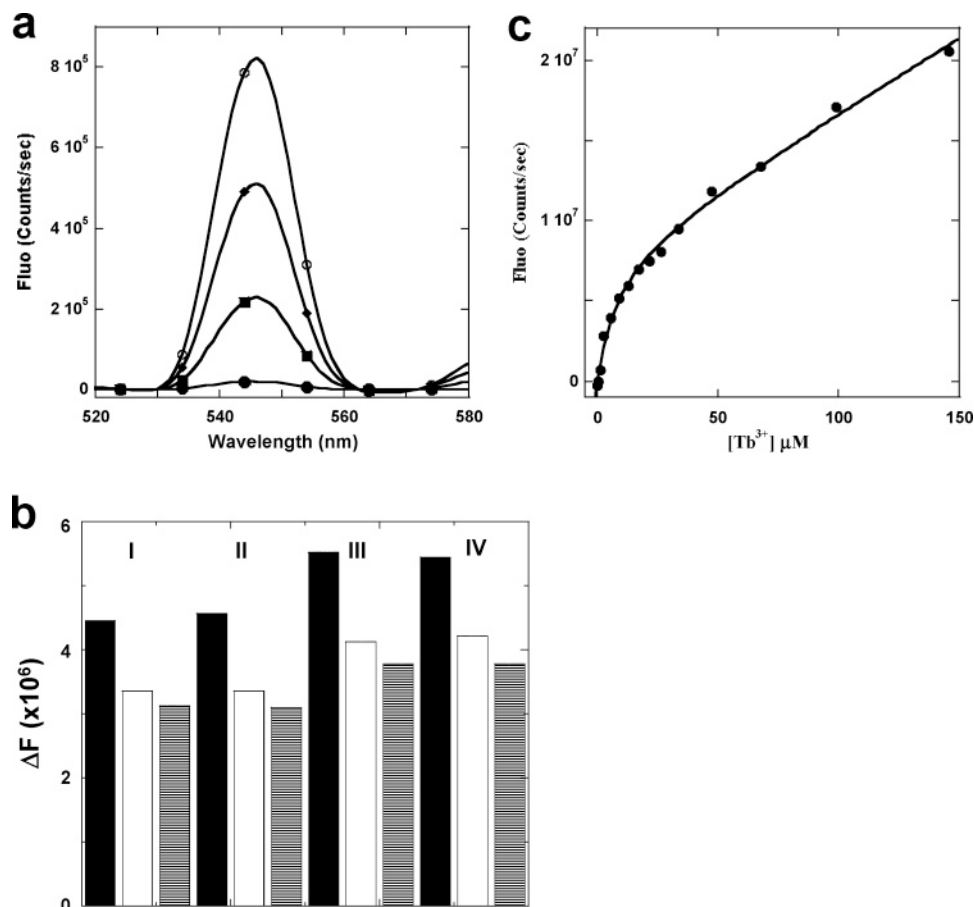
Figure 4. (a) Emission spectra of 20 μM of Tb^{3+} with 0, 6.2, 13.7, and 21.3 (from bottom to top) μM CaM-CD2-I-5G-52 excited at 292 nm. (b) The competition of Tb^{3+} binding by La^{3+} and Ca^{2+}. Tb^{3+} fluorescence enhancement calculated by the integrated area from 525 to 565 nm with 30 μM Tb^{3+} and 20 μM protein in the absence (black bar) and presence of 100 μM La^{3+} (gray bar) or 10 mM Ca^{2+} (horizon) in 10 mM Tris−10 mM KCl, pH 7.4. (c) Fluorescence of CaM-CD2-I-5G-52 with the addition of Tb^{3+}. The intensities of free Tb^{3+} under the same buffer conditions are subtracted from that of the Tb^{3+}−protein mixture samples. The solid line is from model fitting assuming a 1:1 metal−protein complex with additional nonspecific binding (Experimental Methods).
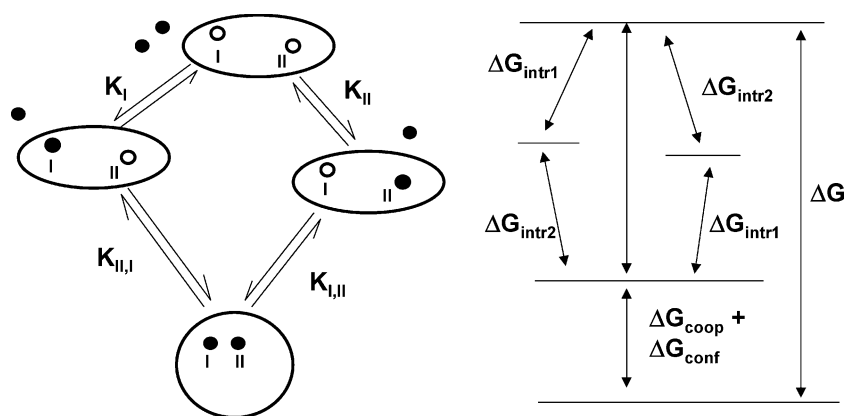

Figure 5. Scheme of Ca^{2+} binding to two coupled EF-hand motifs and Ca^{2+} binding energetics.

where ΔG_{intr1} and ΔG_{intr2} are the free energy changes for forming the 1:1 metal−protein complex resulting from the interaction of the ligand atoms and the metal ion in the coordination shell and the local conformational change of the EF-loop. They are directly related to the microscopic binding constants K_I and K_{II}. ΔG_{conf} is related to the conformational entropy between the apo-forms and loaded forms of each site. It is largely dependent on solvent conditions such as pH, temperature, and salt concentrations.[12,41] ΔG_{coop} is the free energy of interaction (cooperativity) between multiple metal binding sites. Four site-specific binding constants (microscopic), K_I, K_{II}, $K_{I,II}$, $K_{II,I}$, are used to describe the four possible binding steps. The accurate determination of the cooperativity of two-coupled sites requires knowledge of the ratio K_{II}/K_I in addition to two macroscopic association constants K_1 and K_2 or three of the four microscopic binding constants[12] for two possible pathways for binding ions. CaM with four EF-hand motifs in

(41) Akke, M.; Forsen, S.; Chazin, W. J. *J. Mol. Biol.* **1995**, *252*, 102−121.

two tightly coupled domains is more complicated with additional coupling between two domains in addition to their relative contribution of two coupled domains.

Due to the intimate relationship between Ca^{2+}-binding cooperativity and conformational change, obtaining site-specific Ca^{2+}-binding affinity and estimating the cooperativity of CaM and EF-hand proteins are challenging. Previously, site-specific Ca^{2+}-binding affinity data were obtained as a result of the single Tyr residues in the C-terminal domain combined with site-specific mutations.[32] However, the fluorescence signals of these residues also respond to the Ca^{2+}-binding properties of the N-terminal domain.[42] Further, mutations that result in a change of the Ca^{2+}-free state and the Ca^{2+}-bound state of CaM may lead to either an increase or decrease in the Ca^{2+} binding affinity.[26,43−45] Unfortunately, peptide fragments usually lack a well-defined conformation in solutions and have a strong tendency to form dimers or higher aggregates in aqueous solution.[46−49] The Ca^{2+}-binding affinities of isolated Ca^{2+}-binding peptides and fragments of CaM are generally 100−100 000 times weaker than the correlated Ca^{2+} binding sites in the intact proteins.[12,46,50,51] For example, the 12-residue peptide encompassing the EF-loop III of CaM has a Ca^{2+} K_d between 0.8 mM (by Reid and co-workers) and 3 mM (by Borin et al.).[46] Although the incorporation of a disulfide bridge helped to order the structure of the fragment encompassing the helix−turn−helix motif I of *Paramecium tetraurelia* CaM in the presence of Ca^{2+}, it was largely unstructured in the absence of Ca^{2+}.[52]

Using our grafting approach to overcome the complications of cooperativity and global conformational changes, we have obtained, for the first time, the relative intrinsic Ca^{2+}- and Tb^{3+}-binding affinities of the four EF-loops of CaM. Table 1 summarizes the Ca^{2+}, La^{3+}, and Tb^{3+} affinities for the four EF-loops grafted into CD2. EF-loop I has the strongest Ca^{2+}-binding affinity (K_d 34 μM), while loop IV has the weakest (25-fold weaker than that of EF-loop I). EF-loop II and loop III have Ca^{2+}-binding affinities about 7- and 5-fold weaker than that of EF-loop I, respectively. The relative Ca^{2+}-binding affinities of the individual EF-loops of CaM are I > III ≈ II > IV. The same order is observed for both Tb^{3+} and La^{3+} binding. Our results are consistent with results using both direct laser excitation and indirect sensitization of Tb^{3+} luminescence through Tyr residues in CaM. Tb^{3+} and Eu^{3+} bind first to the N-terminal sites with a K_d of 6−12 nM, while K_d values for the weaker sites at the C-terminal end are 2−3 μM.[53,54] Ln^{3+}

ions bind first to sites I and II at the N-terminal of CaM as revealed by NMR.[55,56]

Our relative Ca^{2+} affinities differ from the values predicted from the acid-pair hypothesis of Reid and Hodges.[57] They hypothesized that the relative Ca^{2+}-binding affinity of isolated EF-hand motifs depends on the number and arrangement of the charged ligand residues in the EF-loop (Figure 1).[57] Four acid residues in the coordination sphere provide the most stable arrangement of anionic charges. Two paired, charged ligand residues at both the *x*- and *z*-axes (positions 1 and 9, 5 and 12) provide the best anion pairs because it reduces the dentate−dentate repulsion. As shown in Figure 1, both sites I and IV of CaM have one paired charge on the *z*-axis. Site II has one paired acidic residue on the *x*-axis, and site III of CaM has no paired residues. According to the acid-pair hypothesis, the relative Ca^{2+}-binding affinity of these four sites in CaM is I ≈ IV > II > III. This hypothesis was tested using peptide models[46,47,58,59] and variant proteins.[60,61] Both approaches are limited by global conformational changes and cooperativity (eq 1).

Our studies lead us to propose a charge-ligand-balanced model in which both the number of negatively charged ligand residues (at loop positions 1, 3, 5, 7, 9, and 12) and the balanced electrostatic dentate−dentate repulsion by the adjacent charged residues determine the relative Ca^{2+}-binding affinities. The higher number of negatively charged residues (four versus three) in the coordination sphere stabilizes the protein−Ca^{2+} complex. It is also important to stabilize the conformation of the ligand residues for Ca^{2+} binding even in the apo-form.[62] This stabilization is brought about by reducing the dentate−dentate repulsion with cationic residues. Ligand residue Asp at position 1 and Glu at position 12 of EF-loop are highly conserved and are essential for forming the Ca^{2+}-binding pocket and for maximizing Ca^{2+} affinity. The distances between the charged oxygen atoms of Asp 1 and Glu 12 in the absence and presence of Ca^{2+} are 8.2 and 3.5 Å, respectively. The repulsion between these charged residues is balanced by Ca^{2+} binding. The four EF-loops also contain Asp at position 3, which makes one side of the EF-loop anionic in the apo-form. EF-loop I has the highest Ca^{2+} affinity, which may be a result of both the number of favorably charged ligand numbers and the balancing of the dentate−dentate repulsions. As shown in Table 1, EF-loop I has four charged ligand residues. In addition, two cationic lysine residues at positions 2 and 11 (with a net charge of −2) of the loop provide the stability required for proper Ca^{2+} geometry by neutralizing the repulsion among ligand residues 1, 3, and 12. In contrast, loop IV lacks the positive residue at position 2 to balance the dentate−dentate repulsion between Asp at positions 1 and 3. Loop IV also has an anionic residue, Glu, at position 11 next to the bidentate Glu at position 12. This juxtaposition causes electrostatic repulsion. Both factors desta-

(42) Mukherjea, P.; Maune, J. F.; Beckingham, K. *Protein Sci.* **1996**, *5*, 468−477.
(43) Li, M. X.; Gagne, S. M.; Spyracopoulos, L.; Kloks, C. P.; Audette, G.; Chandra, M.; Solaro, R. J.; Smillie, L. B.; Sykes, B. D. *Biochemistry* **1997**, *36*, 12519−12525.
(44) Henzl, M. T.; Hapak, R. C.; Likos, J. J. *Biochemistry* **1998**, *37*, 9101−9111.
(45) Fefeu, S.; Biekofsky, R. R.; McCormick, J. E.; Martin, S. R.; Bayley, P. M.; Feeney, J. *Biochemistry* **2000**, *39*, 15920−15931.
(46) Borin, G.; Ruzza, P.; Rossi, M.; Calderan, A.; Marchiori, F.; Peggion, E. *Biopolymers* **1989**, *28*, 353−369.
(47) Reid, R. E. *J. Biol. Chem.* **1990**, *265*, 5971−5976.
(48) Shaw, G. S.; Hodges, R. S.; Sykes, B. D. *Science* **1990**, *249*, 280−283.
(49) Franchini, P. L.; Reid, R. E. *J. Theor. Biol.* **1999**, *199*, 199−211.
(50) Drabikowski, W.; Brzeska, H.; Venyaminov, S. *J. Biol. Chem.* **1982**, *257*, 11584−11590.
(51) Reid, R. E. *Biochemistry* **1987**, *26*, 6070−6073.
(52) Le Clainche, L.; Plancque, G.; Amekraz, B.; Moulin, C.; Pradines-Lecomte, C.; Peltier, G.; Vita, C. *J. Biol. Inorg. Chem.* **2003**, *8*, 334−340.
(53) Mulqueen, P.; Tingey, J. M.; Horrocks, W. D., Jr. *Biochemistry* **1985**, *24*, 6639−6645.
(54) Bruno, J.; Horrocks, W. D., Jr.; Zauhar, R. J. *Biochemistry* **1992**, *31*, 7016−7026.
(55) Bertini, I.; Gelis, I.; Katsaros, N.; Luchinat, C.; Provenzani, A. *Biochemistry* **2003**, *42*, 8011−8021.
(56) Hu, J.; Jia, X.; Li, Q.; Yang, X.; Wang, K. *Biochemistry* **2004**, *43*, 2688−2698.
(57) Reid, R. E.; Hodges, R. S. *J. Theor. Biol.* **1980**, *84*, 401−444.
(58) Reid, R. E.; Clare, D. M.; Hodges, R. S. *J. Biol. Chem.* **1980**, *255*, 3642−3646.
(59) Marsden, B. J.; Hodges, R. S.; Sykes, B. D. *Biochemistry* **1988**, *27*, 4198−4206.
(60) Wu, X.; Reid, R. E. *Biochemistry* **1997**, *36*, 8649−8656.
(61) Black, D. J.; Tikunova, S. B.; Johnson, J. D.; Davis, J. P. *Biochemistry* **2000**, *39*, 13831−13837.
(62) Christensen, T.; Gooden, D. M.; Kung, J. E.; Toone, E. J. *J. Am. Chem. Soc.* **2003**, *125*, 7357−7366.

bilize the apo-form of the Ca^{2+} binding loop IV leading to the weakest binding. The Ca^{2+} affinity of loop III is moderate because it has only three negatively charged residues, although Lys at position 2 provides some stability for the apo-form. On the other hand, EF-loop II has four negatively charged ligand residues but lacks positively charged residues to neutralize the electrostatic repulsion.

Our data suggest that the stronger Ca^{2+}-binding affinity of the C-terminal domain of CaM compared to the N-terminal domain in the intact protein is from cooperativity and confor-mational changes in the C-terminal rather than stronger intrinsic metal affinity. Several other observations support this hypothesis. For example, the C-terminal, especially site IV, is less structured in the apo-CaM.[63] The thermal stability of the C-terminal domain of apo-CaM is lower than that of the N-terminal domain.[64] These observations suggest that the C-terminal undergoes a greater conformational change upon Ca^{2+} binding. The 1D NMR study also shows that the cooperativity from the C-terminal domain is higher than that of the N-terminal domain.[65] In the same study, a difference in binding free energy of ~4.2 kJ/mol was observed between the two binding sites in the N-terminal of CaM,[65] which is consistent with the affinity difference observed for site I and site II. Based on our Ca^{2+} binding data (Table 1), site I binds Ca^{2+} more tightly by 2.8 kJ/mol at pH 6.8 and 4.9 kJ/mol at pH 7.4. Furthermore, removing the hydrophobic interaction between loop III and IV (V136G) results in Ca^{2+} binding to the N-terminal domain prior to the C-terminal.[66] Because the intrinsic Ca^{2+}-binding affinity difference between C-terminal and N-terminal domains is less than 7.2 kJ/mol, these results indicate that cooperativity and conformational change determine the Ca^{2+}-binding order in CaM.

4.2. Contribution of Cooperativity and Conformational Change. At pH 7.5 and in a low salt buffer, the two macroscopic Ca^{2+} binding at the N-terminal domain of CaM (TR_1C) are 37.45 and 37.34 kJ/mol, respectively, while those at the C-terminal domain (TR_2C) are 39.39 and 43.96 kJ/mol, respec-tively.[25] Using recombinant expressed TR_1C and TR_2C with trimethylated Lys-115, the two macroscopic dissociation con-stants for TR_2C are slightly decreased, while that for TR_1C is not changed.[26] The cooperativity of CaM has been estimated by Linse et al. assuming the identity of sites I and II or sites III and IV.[25] Assuming the conformation of CD2 is not changed upon Ca^{2+} binding (Figure 2a) and the influence of the Gly linker of the host protein is negligible, we can estimate the contribution of cooperativity and conformational change from other parts of CaM as −28.58 and −40.21 kJ/mol for the N- and C-terminal domains, respectively. The contribution of the

cooperativity and conformational change to the Ca^{2+} affinity for the C-terminal is 40% greater than that for the N-terminal. The large contributions of cooperativity and conformational change we obtained here could be due to the summation of contributions toward stabilization made by additional structural units such as the flanking helices and their packing and interaction, as well as by hydrophobic interaction between the small β-sheets of two coupled EF-loops. The conformational change and cooperativity between two sites may alter the k_{on} rate of the second site and the k_{off} rates of both sites, which increase their apparent binding affinities. As shown in Table 1, the Ca^{2+} affinities of each individual EF-loop in CaM are about 10−50-fold smaller in the scaffold protein than the averaged Ca^{2+} affinity of individual domains (0.3−3.0 μM). Our data suggest that the greater cooperativity and conformational changes of protein surroundings result in higher Ca^{2+} affinity as a coupled C-terminal domain than that of the N-terminal domain.

In summary, we have shown that the insertion of single EF-loops I, II, III, and IV does not change the structure of the host protein, CD2. Like the CaM, the isolated EF-loops I, II, III, and IV bind Ca^{2+}, Tb^{3+}, and La^{3+}. Using a grafting approach, we have shown site-specific Ca^{2+} affinities of the individual EF-hand loops of CaM decrease in the order I > III $\approx$ II > IV. This order also holds for La^{3+} and Tb^{3+}. Our results suggest that both the number of negatively charged ligand residues and the balanced electrostatic dentate−dentate repulsion by the adjacent charged residues are major determinants for Ca^{2+}-binding affinities of EF-loops. Our grafting method can be used to obtain and predict site-specific Ca^{2+}-binding affinities of other EF-hand proteins and provides a better estimation of the contribution of the cooperativity and conformational change for coupled Ca^{2+}-binding sites. These findings are an important advance in understanding how EF-hand proteins use the ubiquitous EF-hand Ca^{2+}-binding motif to coordinate diverse cellular functions and how Ca^{2+} binding regulates the biological functions of trigger/sensor proteins such as CaM in the Ca^{2+}-signaling cascade.[16]

Supporting Information Available: Supporting fluorescence and NMR results. This material is available free of charge via the Internet at http://pubs.acs.org.

JA042786X

(63) Kuboniwa, H.; Tjandra, N.; Grzesiek, S.; Ren, H.; Klee, C. B.; Bax, A. *Nat. Struct. Biol.* **1995**, *2*, 768−776.
(64) Protasevich, I.; Ranjbar, B.; Lobachov, V.; Makarov, A.; Gilli, R.; Briand, C.; Lafitte, D.; Haiech, J. *Biochemistry* **1997**, *36*, 2017−2024.
(65) Pedigo, S.; Shea, M. A. *Biochemistry* **1995**, *34*, 10676−10689.
(66) Abagyan, R. A. *FEBS Lett.* **1993**, *325*, 17−22.
(67) Kraulis, P. J. *J. Appl. Crystallogr.* **1991**, *24*, 946−950.